A Study on IF Signal Fading in the Fiber-Optic Millimeter Wave System Using Self-Heterodyne Methods

Sung-Kweon Park

The Graduate School
Yonsei University
Department of Electrical and Electronic Engineering

A Study on IF Signal Fading in the Fiber-Optic Millimeter Wave System Using Self-Heterodyne Methods

A Master's Thesis
Submitted to the Department of Electrical and Electronic Engineering
and the Graduate School of Yonsei University
in partial fulfillment of the
requirements for the degree of
Master of Science

Sung-Kweon Park

June 2005

This certifies that the master′s thesis of Sung-Kweon Park is approved.

_____

Thesis Supervisor: Woo-Young Choi

_____

Sang-Kook Han

_____

June-Koo Rhee

The Graduate School

Yonsei University

June 2005

Contents

Figure Index

Table Index

Abstract

A Study on IF Signal Fading in the Fiber-Optic Millimeter Wave System Using Self-Heterodyne Methods

By

Sung-Kweon Park

Department of Electrical and Electronic Engineering

The Graduate School

Yonsei University

Recently, of great interest to end user is the millimeter wave band which provides wireless access to broadband network. Especially, the millimeter wave band of 60GHz will be used in the foreseeable future. It has enormous merits in the view of technology and economics to use fiber-optic transmission systems between the central station and the base station. In this thesis, a study on IF signal fading is done in the fiber-optic 60GHz millimeter wave system using self-heterodyne methods.

Single-mode fiber, also called “legacy fiber,” has the chromatic dispersion and the polarization mode dispersion effect which can result in signal fading (or power penalty) on the received millimeter wave. However, the dispersion effect is not too

serious because practical range of fiber-optic transmission is less than 20km as well as the various dispersion compensation techniques are available.

On the other hand, the random changes in refractive index of the optical fiber due to environmental conditions such as temperature, stress, and vibration can cause the down-converted IF signal in the mobile station to fade with time, which is defined here as IF signal fading. Through the analysis in this thesis, the IF signal fading problem can be considerably alleviated by inserting the 60GHz bandpass filter after the photodiode. This filter only selects the upper sideband of the received millimeter wave and rejects other image components.

Based on the solution for the IF signal fading problem, the system performance is demonstrated with 16QAM data modulation and 20km fiber length. 60GHz millimeter wave is successfully generated and down-converted to the 1GHz IF band without IF signal fading.

Keywords: millimeter wave, self heterodyne, IF signal fading, DSB-SC, fiber-optic transmission, chromatic dispersion, fiber ambient effect, thermo-optic effect

I. Introduction

Future wireless access to broadband networks will provide the user both high-speed data and enormous bandwidth [1]. The frequency band around 60GHz will be a promising and reasonable candidate to the access network [2]. As shown in Figure 1-1, various wireless services such as interactive multimedia service (IMS), intelligent traffic service (ITS) and broadband mobile service will allocate the frequency band around 60GHz or the millimeter wave band in the foreseeable future. At this frequency band, however, the characteristics of wireless channels are so harsh that the designer of the network architecture should consider the micro/pico cells. Moreover, the smaller the cell size is, the more remote antenna units (RAUs) are needed to cover large service area with radio access.

In the view of economics, of great importance is the compact and cost-efficient RAU, which enables the fast deployment of brand-new technologies [3]. And the signal loss and attenuation during the transmission between the central station (CS) and the base station (BS) should be as small as possible. It would be just the thing to use the optical fiber links for high capacity and low attenuation. As can be seen in Figure 1-2, optical generation and transmission of the millimeter wave over optical fiber links is mandatory and several techniques have been proposed since the 1990s [4]-[9].

The fiber-optic transmission links, however, have many detrimental factors to the signal qualities. Chromatic dispersion, polarization mode dispersion (PMD), laser phase noise, amplified spontaneous emission (ASE) noise, fiber ambient effects, and fiber nonlinearities are the limiting factors to the system performances such as bit error rate or signal to noise ratio. Some factors cause the received signal to fade or fluctuate with time in a phenomenological viewpoint. The phenomenon of the signal fading can result in the increase of the bit error rate. Thus, a variety of studies on the detrimental factors of the fiber-optic links have been performed [10]-[13].

In this thesis, the fiber-optic optical millimeter wave system using optical self heterodyne detection method is theoretically analyzed and experimentally demonstrated. Before the analysis of the subject, the optical self heterodyne detection method is explained in chapter II. Then, especially focused on the fading of the IF signal in the mm-wave systems, the origin and the solution of the IF signal fading are theoretically and experimentally analyzed in the chapter III. Some conclusions are presented in chapter IV.

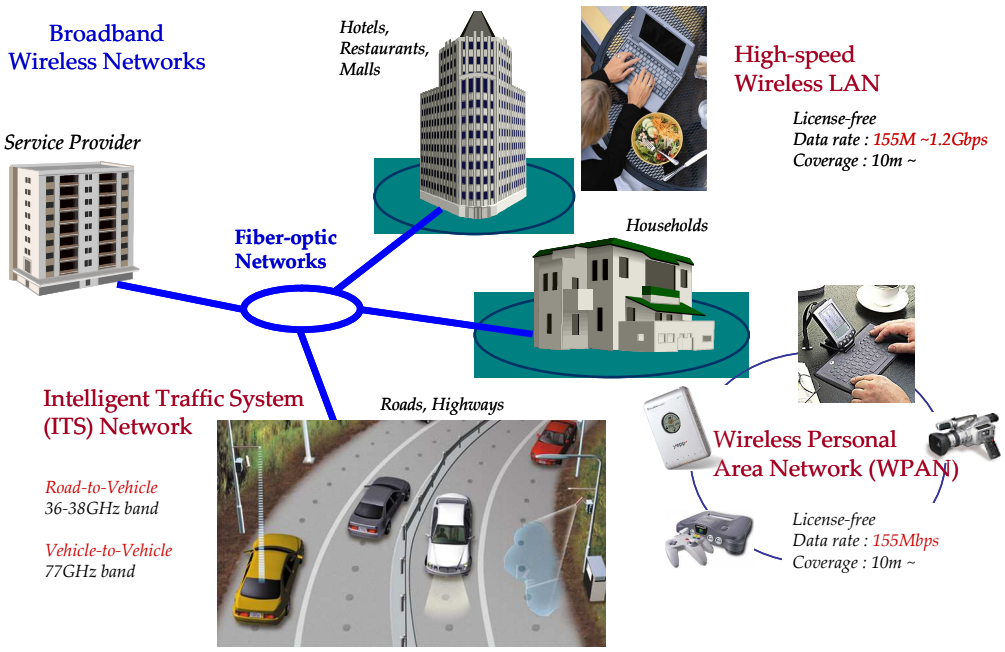

Figure 1-1 Wireless services using 60GHz millimeter wave

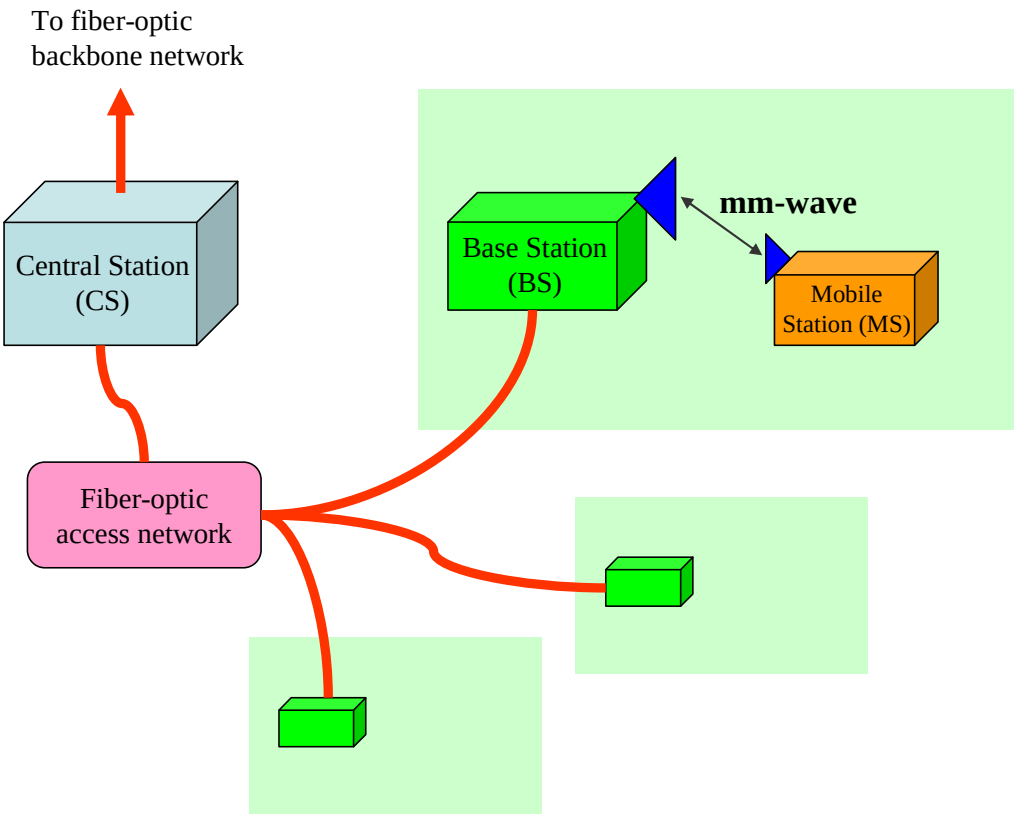

Figure 1-2 Fiber-optic mm-wave wireless access network

II. Optical Self Heterodyne Detection Methods

1. Basic Concept

In this thesis, 60GHz millimeter wave is optically generated by optical self heterodyne detection method. Two phase-correlated optical carriers, at frequencies f_1 and f_2 that are offset by the desired millimeter wave frequency, are generated in the transmitter. These two optical carriers are transported through the optical fiber and detected by a photodiode. By the square-law detection of the photodiode, the desired millimeter wave carrier can be generated. Fig. 2-1 depicts the concept of the optical generation of the millimeter wave by optical self heterodyne detection method. The name, self heterodyne, means that the up-conversion of the IF data to the millimeter-wave frequency band can be implemented not by additional local oscillators but by the beating of two phase-correlated optical carriers.

For the generation of two optical carriers, the dual-frequency laser transmitters are required and can be implemented in various ways [14]. In this thesis, lithium niobate ($LiNbO_3$) Mach-Zehnder modulator (MZM) that can operate up to 40GHz is used. The transfer curve of MZM is shown in Fig. 2-2. The transfer function of MZM is expressed by

$$I_{out}(t) = \alpha I_{in} \cos^2\left(\frac{\pi}{2V_\pi} V(t)\right) \tag{2-1}$$

where $I_{out}(t)$ denotes the transmitted intensity, α the insertion loss, I_{in} the input intensity, $V(t)$ the applied voltage, and V_{π} the driving voltage. In the Eqn. 2-1, $V(t)$ consists of the DC bias and the AC modulating signal. According to the DC bias, there are three bias points as shown in Fig. 2-2, which are minimum transmission bias (MITB) point, quadrature bias (QB) point, and maximum transmission bias (MATB) point, respectively. In order to generate two optical carriers for the optical self heterodyne method, the MZM should be operated in the minimum transmission bias point.

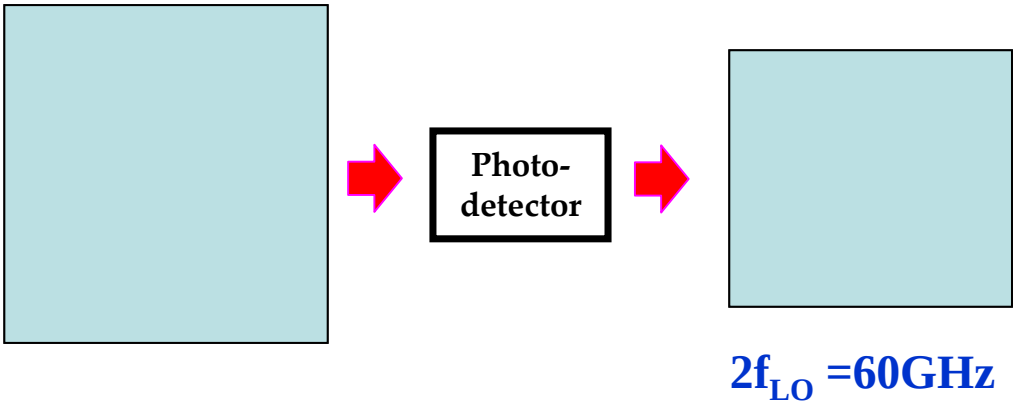

Figure 2-1 Concept of the optical self heterodyne detection method

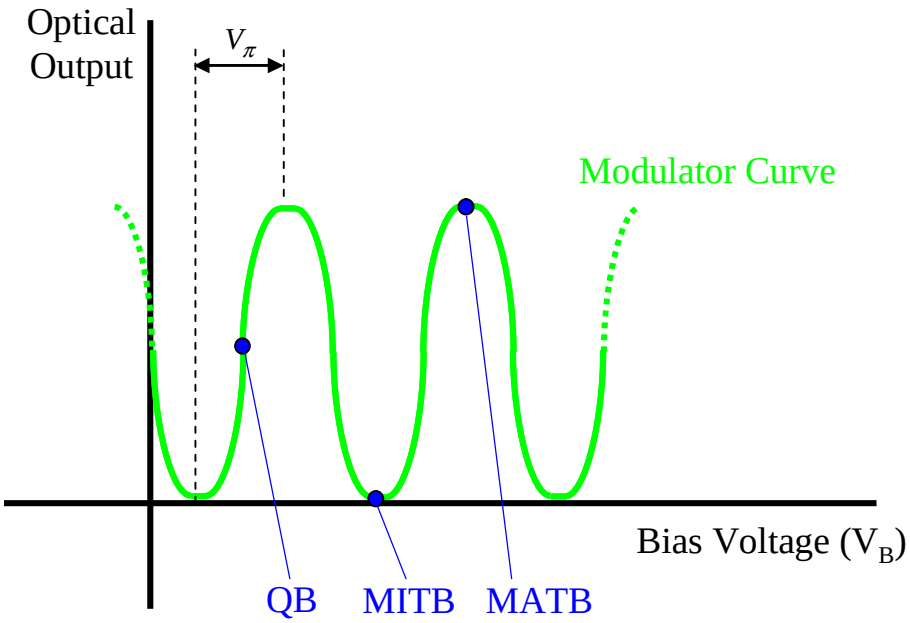

Figure 2-2 Modulator curve of the Mach-Zehnder modulator (MZM)

QB : Quadragure Bias

MITB : Minimum Transmission Bias

MATB : Maximum Transmission Bias

2. Optimum Conditions for the Generation of Dual Optical Carriers

For the generation of dual optical carriers of which frequencies are offset by the desired millimeter wave frequency, as mentioned previously, the MZM must be operated in the minimum transmission bias point. In this section, the optimum condition for optical self heterodyne detection method is discussed theoretically with focusing on the modulation efficiency.

The electrical field of the MZM output is expressed by

$$E_{out}(t) = E_{in} \cos\left(\frac{\pi}{2V_{\pi}} V(t) \right) e^{j\omega_o t} \tag{2-2}$$

where $E_{out}(t)$ denotes the output field intensity, E_{in} the input field intensity, $V(t)$ the applied voltage, V_{π} the driving voltage, and ω_o the optical carrier frequency from the laser source. $V(t)$ consists of the DC bias and the AC modulating signal, and can be given by

$$V(t) = V_{DC} + V_{AC} \cos \omega_{RF} t \tag{2-3}$$

where V_{DC} denotes the DC bias voltage, V_{AC} the RF signal voltage, and ω_{RF} the frequency of the RF modulating signal. In Eqn. 2-3, the modulating signal is an analog RF carrier.

Substituting Eqn. 2-3 into Eqn. 2-2,

$$
\begin{aligned}
E_{out}(t) &= E_{in}\cos\left(\frac{\pi V_{DC}}{2V_\pi}+\frac{\pi V_{AC}}{2V_\pi}\cos\omega_{RF}t\right)\cos\omega_o t \\
&= E_{in}\left[\cos\frac{\pi\alpha_{DC}}{2}\cos\left(\frac{\pi\alpha_{AC}}{2}\cos\omega_{RF}\right)-\sin\frac{\pi\alpha_{DC}}{2}\sin\left(\frac{\pi\alpha_{AC}}{2}\cos\omega_{RF}t\right)\right]\cos\omega_o t \\
&= E_{in}\cos\frac{\pi\alpha_{DC}}{2}\sum_{n=-\infty}^{\infty}(-1)^n J_{2n}(\frac{\pi\alpha_{AC}}{2})\cos[2n\omega_{RF}t]\cos\omega_o t \\
&\quad - E_{in}\sin\frac{\pi\alpha_{DC}}{2}\sum_{n=-\infty}^{\infty}(-1)^{n-1} J_{2n-1}(\frac{\pi\alpha_{AC}}{2})\cos[(2n-1)\omega_{RF}t]\cos\omega_o t \\
&= E_{in}\cos\frac{\pi\alpha_{DC}}{2}J_0(\frac{\pi\alpha_{AC}}{2})\cos\omega_o t \\
&\quad - E_{in}\sin\frac{\pi\alpha_{DC}}{2}J_1(\frac{\pi\alpha_{AC}}{2})\cos(\omega_o\pm\omega_{RF})t \\
&\quad - E_{in}\cos\frac{\pi\alpha_{DC}}{2}J_2(\frac{\pi\alpha_{AC}}{2})\cos(\omega_o\pm 2\omega_{RF})t \\
&\quad + E_{in}\sin\frac{\pi\alpha_{DC}}{2}J_3(\frac{\pi\alpha_{AC}}{2})\cos(\omega_o\pm 3\omega_{RF})t \\
&\quad +\cdots
\end{aligned}
\tag{2-4}
$$

where $\alpha_{DC}=V_{DC}/V_\pi$ is the normalized bias level, $\alpha_{DC}=V_{DC}/V_\pi$ the normalized drive level, and $J_n(\cdot)$ the nth-order Bessel function of the first kind.

From the last expression of Eqn. 2-4, the electrical fields of the MZM output are composed of fundamental-mode optical carrier and other sideband modes which are separated by the frequency of the drive RF signal. The normalized bias level, α_{DC}, determines the operating point of the MZM and has particular interest when α_{DC} is the value of 0, 0.5, and 1. Firstly, when α_{DC} is 0, all odd modes are suppressed,

which is the case of maximum transmission bias point. When α_{DC} is 0.5, this is the case of quadrature bias point in which an optical carrier is linearly modulated. Finally, when α_{DC} is 1, both fundamental-mode optical carrier and even modes are suppressed and odd modes including first-mode carriers are transferred, which is the case of minimum transmission bias point. In the minimum bias point, fundamental-mode optical carrier is suppressed and most of the power is transferred to the first-mode sidebands, upper sideband and lower sideband. So, this is the form of the double sideband with suppressed carrier (DSB-SC). And the DSB-SC enables the dual phase-correlated optical carriers which are adoptable for the optical self heterodyne detection method. For example, if f_{RF} =30GHz under the minimum bias point, two first-mode sidebands are separated by 60GHz. When these are detected in a photodiode, 60GHz millimeter wave can be obtained.

On the other hand, the intensity of the two first-mode sidebands depends on the bias voltage level (V_{DC}) and the RF signal voltage level (V_{AC}). Since the bias voltage level determines the operating point of the MZM, it should be constant. If necessary, a modulator bias controller which makes the modulator bias point stable can be used. Thus, the optimum condition that provides the two first-mode sidebands with maximum power depends on the drive signal voltage level. More precisely, the power of the first-mode sideband is directly proportional to $J_1(\frac{\pi\alpha_{AC}}{2})$. Therefore, the optimum condition for maximum modulation efficiency is determined when the 1st -order Bessel function, $J_1(x)$, is maximum.

$$J_n(x) = \sum_{r=0}^{\infty} \frac{(-1)^r (x/2)^{n+2r}}{r!\Gamma(n+r+1)} \tag{2-5}$$

With simple numerical analysis of Eqn. 2-5, $J_1(x)$ is maximum when the variable of the 1st-order Bessel function, x, is 1.84. In Eqn. 2-5, $x = \frac{\pi\alpha_{AC}}{2} = \frac{\pi V_{AC}}{2V_\pi} = 1.84$.

Thus, that $V_{AC} = 1.17V_\pi$ is the optimum condition of the drive signal voltage level. Since the modulator drive voltage (V_π) has generally the range between 4V and 6V, if assuming 5V, the RF signal voltage level (V_{AC}) is 5.85V which is equivalent to 25.3dBm of RF power. In conclusion, the drive RF amplifier should be used in the experiment because maximum output power of the RF signal source we have is lower than 8dBm.

III. IF Signal Fading

As depicted in Fig. 2-1 and discussed in chapter II, the dual optical carriers with IF data are generated in the central station (CS) and transported to the base station (BS) over optical fibers. In the BS, the millimeter wave (mm-wave) is generated by a photodiode and radiated by an antenna. This millimeter wave arrives at the mobile station (MS) and is down-converted to the IF band by one or more local oscillators.

The full-link experiment shows a critical problem that the power of the donw-converted IF signal periodically fluctuates, which is defined as the IF signal fading in this thesis. The phenomenon of the IF signal fading is described in the first section. And in the following section, the cause of the IF signal fading is discussed theoretically and experimentally. In the final section, the solution for the IF signal fading is suggested and demonstrated with 16 QAM IF data.

1. Full-link Experimental Setup

A. Central station

The experimental setup is shown in Fig. 3-1. For generating 60GHz mm-wave, 30GHz RF signal, denoted by f_{LO}, is used. In this experiment, the IF signal is the 1.5GHz RF carrier which does not include baseband data and is denoted by f_{IF}. The RF mixer is used for modulating the f_{LO} with the f_{IF}. After the mixing of the two RF signal, a double sideband (DSB) signal centered at the $f_{LO} = 30GHz$ is

generated. The DSB signal modulates the 1550nm of a CW light in the minimum bias point of the MZM. The CW light source is fed from the tunable laser source. As discussed in chapter II, the drive amplifier is placed between the RF mixer output and the MZM RF input for the optimum bias condition which makes the output with maximum power. As a result of the modulation in the MZM, the six field components are generated.

B. Fiber-optic channel

The fiber-optic channel is simply composed of the single mode fiber (SMF) and the erbium doped fiber amplifier (EDFA). The SMF has the dispersion D=17 ps/nm·km and the length of 20km. The length of the fiber-optic link between the CS and the BS will be as short as 20km or less in that the cell size is considered to be very small. Therefore, the length of 20km is reasonable for the system experiment. However, the SMF which is used in this experiment is bound to a fiber spool and exposed in the air without any coating. So, the SMF can be affected by a variety of environmental factors. On the other hand, the EDFA is placed just rear of the MZM for boosting the weak optical signal.

C. Base station

The base station (BS) consists of the 60GHz photodiode (PD) and amplifier. The millimeter wave detected by the PD is so weak in power that the 60GHz RF

amplifier is used. The 3dB gain bandwidth of the RF amplifier is about 1GHz. The BS in this experiment does not have any antenna for radiating the mm-wave. Thus, the detected mm-wave is transported to the mobile station through the rectangular RF waveguide. The detected mm-wave is monitored in the RF Spectrum analyzer.

D. Mobile station

In the mobile station (MS), the mm-wave is down-converted to the IF band for an additional processing. Since the IF signal is plainly RF carrier without data, there is no additional processing. For down-converting the 60GHz mm-wave to the IF band, the sub-harmonic mixer is used. The sub-harmonic mixer performs the down-conversion with 30GHz LO signal (f_{LO}) which is fed by the RF source in the central station. The down-converted IF signal is monitored in the RF spectrum analyzer. RF phase shifter is placed in order to maximize the power of the IF signal.

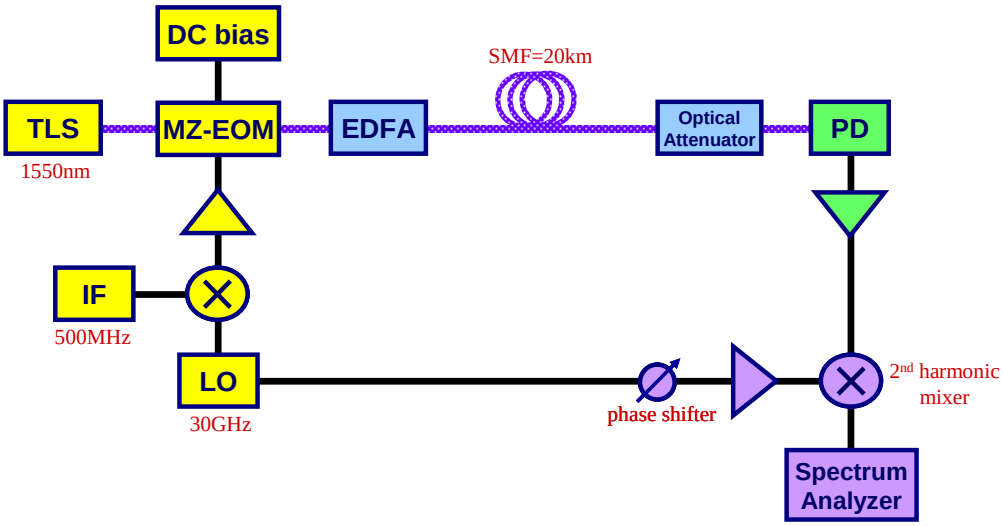

Figure 3-1 Experimental setup

TLS : Tunable Laser Source

MZ-EOM : Mach-Zehnder electro-optic modulator

EDFA : Erbium-doped fiber amplifier

PD : Photodiode

2. Results of the experiment

A. RF phase shifter

In the experiment, the RF phase shifter is used to maximize the power of the IF signal because the phase difference exists in the 30GHz local oscillators between the CS and MS. The 30GHz local oscillator in the CS is used to modulate the optical carrier and make dual optical carrier which is separated by 60GHz as discussed in chapter II. On the other hand, the 30GHz local oscillator in the MS is used to down-convert 60GHz millimeter wave into the IF band. Sub-harmonic mixer performs this down-conversion process. Practically, only one 30GHz local oscillator is used because the 30GHz RF source is shared in both CS and MS. However, the phases of the millimeter wave and the 30GHz LO signal in the MS are not same because the fiber-optic transmission. Therefore, the RF phase shifter in the MS can compensate for the phase difference and the IF signal is maximized.

B. IF signal fading

Fig. 3-2 shows the spectrum of the IF signal whose frequency is lied on the IF band. But the power of the IF signal fluctuates with time, which is defined as the IF signal fading. The IF signal is completely faded with a time period. The period depends on the time when the experiment is performed and the fiber length. Though the dependence of IF band frequency and power which is applied in the transmitter or the bias condition which explains the degree of the suppression of the center carrier in the MZM are examined, those parameters have a little effect on the period

of the IF signal fluctuation. The period of the IF signal fluctuation is shown in Table 3-1, 3-2, and 3-3.

Table 3-1 shows the result of the dependence of fiber length on the fading period. As the fiber length increases, the fading period is shortened and the phenomenon of the fluctuation makes worse the system performance. Table 3-2 shows the result of the dependence of bias voltage on the fading period. According to the bias voltage, the suppression of the fundamental mode varies, which causes the power ratio of the fundamental mode and first mode to vary, too. However, the condition of the bias voltage does not have considerable effect on the fading period. Table 3-3 also shows that the IF carrier frequency does not have influence on the fading period. From the experimental results of the fading period, the longer the fiber length, the more effect of fiber ambient conditions is observed.

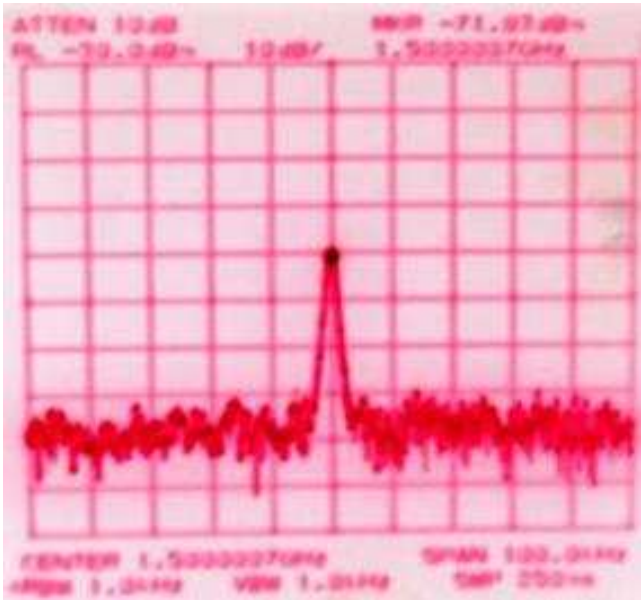

Figure 3-2 IF signal spectrum (1.5GHz)

Fiber length	Bias condition	Period (s)
5km	5.4V (104.8/32.3)	5min., 5min., 4min,...
10km	5.4V (125.6/38.3)	150, 140, 160,...
20km	5.4V (100.9/30.1)	65, 53, 50, 60, 55, 52, 55, 55,...
25km	5.4V (71/21) PD=−2dBm	47, 58, 65, 57, 46, 51, 50, 54,...

Table 3-1 Fiber length dependence

Fiber length	Bias condition (suppression ratio)	Period (s)
20km	4.9V (88/68)	49, 48, 48, 49,...
20km	5.0V (93.5/54)	51, 52, 51, 49,...
20km	5.4V (100.9/30.1)	51, 52, 55, 55,...

Table 3-2 Bias voltage dependence

Bias	IF Freq. (MHz)	Period (m)	Detected IF Power Range
5.2V (163/50.5)	50	5, 5, 5, ...	−52 ~ −75 dBm
5.2V (164/51.4)	100	5, 5, 4.5, ...	−54 ~ −82 dBm
5.2V (162/50.8)	500	5, 6, 6, ...	−55 ~ −70 dBm

Table 3-3 IF carrier frequency dependence (fiber length=20km)

3. Analysis on the IF Signal Fading

As discussed in the previous section, according to the environmental conditions and other experimental parameters, the period of the IF signal fading varies from 1 minute to 20 minutes or so. And the power of the IF signal fluctuates from -30 dBm to -60 dBm or so. Coincidentally, the power is varied in the same range if manually adjusting the RF phase shifter. Therefore, the phenomenon of the IF signal fading is originated from the phase drift of the millimeter wave which is arrived at the mobile station. This phase drift causes the phase difference in the local oscillator between the CS and the MS to vary with time, and the power of the IF signal also varies with time. The phase drift of the millimeter wave is a direct origin of the IF signal fading. And the phase drift is closely related with the changes in the effective length of the optical fiber. The real length of the optical fiber is fixed to 20km in the experiment. But, the effective length of the optical fiber can change if the refractive index of the fiber varies due to the environmental conditions such as ambient temperature, stress and mechanical vibration. This variation of the effective fiber length causes the arrival time of the millimeter wave to vary with time. Thus, the phase drift of the millimeter wave can occur in the system.

In this section, the phase drift of the millimeter wave and the amplitude drift (or signal fading) of the down-converted IF signal are theoretically analyzed. And then the effect of the ambient temperature on the IF signal fading is considered theoretically and experimentally.

A. Theoretical analysis

Here, theoretically analyzed is the phase drift of the received mm-wave signal in the BS and the IF signal fading in the MS. It should be stressed that the signal fading occurs not in the mm-wave band but in the IF band. Assuming that fiber dispersion effects such as chromatic dispersion and polarization mode dispersion are compensated, the 6 field components after the fiber transmission of the length L are expressed as follows.

$$E_i^{fiber}(t) = A_i e^{j(\omega_i t - \phi_i)} = A_i e^{j(\omega_i t - k_i L)} = A_i e^{j\left(\omega_i t - \frac{\omega_i L \cdot n(t)}{c}\right)} \quad \text{i=1, 2, … 6} \qquad (3\text{-}1)$$

In Eqn. 3-1, ω_i is the carrier frequency.

$$\omega_1 = \omega_o - \omega_{LO} - \omega_{IF}$$

$$\omega_2 = \omega_o - \omega_{LO}$$

$$\omega_3 = \omega_o - \omega_{LO} + \omega_{IF}$$

$$\omega_4 = \omega_o + \omega_{LO} - \omega_{IF}$$

$$\omega_5 = \omega_o + \omega_{LO}$$

$$\omega_6 = \omega_o + \omega_{LO} + \omega_{IF} \qquad (3\text{-}2)$$

k_i is the propagation constant and $\phi_i = k_i L$ means the delayed phase induced by fiber-optic transmission. The refractive index, $n(t)$, is the function of the fiber ambient effects such as temperature change, mechanical stress, vibration, and so on.

Therefore, the refractive index becomes the function of time, i.e. a random variable. Especially, ambient temperature effect is considered in the following subsection B. The fact that the refractive index is not the constant but the function of time is the key to explain the phase drift of the mm-wave and the IF signal fading.

In the antenna base station, the above six field components are detected by a photodiode and 3 mm-wave components are obtained as depicted in Fig. 3-3.

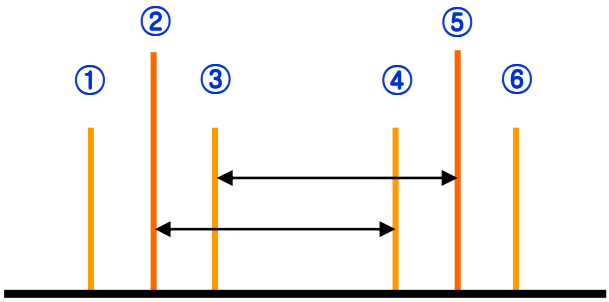

(a) Lower sideband ($\omega_7 = 2\omega_{LO} - \omega_{IF}$)

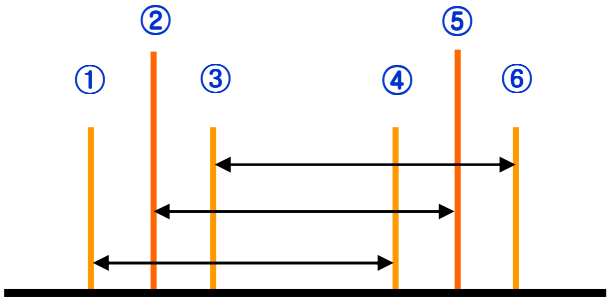

(b) Center carrier ($\omega_8 = 2\omega_{LO}$)

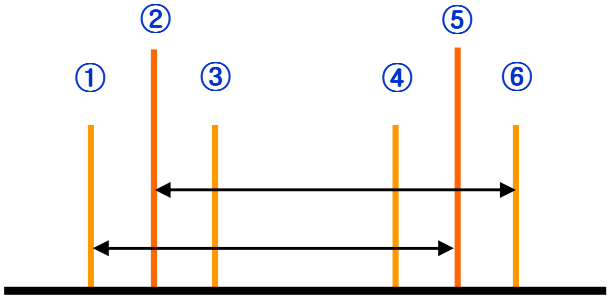

(c) Upper sideband ($\omega_9 = 2\omega_{LO} + \omega_{IF}$)

Figure 3-3 Demonstration of the beating of the 6 optical fields

After photo-detection in the antenna base station, the three mm-wave components are expressed as follows.

$$
\begin{aligned}
& I_7^{PD}(t) \\
& = \Re(E_2 E_4^* + E_2^* E_4) + \Re(E_3 E_5^* + E_3^* E_5) \\
& = 2\Re A_{LO} A_{IF} \left[\cos(\omega_7 t - \delta_4 + \delta_2) + \cos(\omega_7 t - \delta_5 + \delta_3)\right] \\
& = 2\chi\Re A_{LO} A_{IF} \left[\cos\left(\omega_7 t + \frac{(\omega_2 - \omega_4) L \cdot n(t)}{c}\right) + \cos\left(\omega_7 t + \frac{(\omega_3 - \omega_5) L \cdot n(t)}{c}\right)\right]
\end{aligned}
$$

Since $\omega_2 - \omega_4 = \omega_3 - \omega_5 = \omega_{IF} - 2\omega_{LO}$,

$$
\begin{aligned}
& = 4\Re A_{LO} A_{IF} \cos\left(\omega_7 t + \frac{(\omega_{IF} - 2\omega_{LO}) L \cdot n(t)}{c}\right) \\
& = 4\Re A_{LO} A_{IF} \cos(\omega_7 t + \phi_7)
\end{aligned}
\qquad \text{(3-3)}
$$

$$
\begin{aligned}
& I_8^{PD}(t) \\
& = \Re(E_1 E_4^* + E_1^* E_4) + \Re(E_2 E_5^* + E_2^* E_5) + \Re(E_3 E_6^* + E_3^* E_6) \\
& = 2\Re A_{IF}^2 \left[\cos(\omega_8 t - \delta_4 + \delta_1) + \cos(\omega_8 t - \delta_6 + \delta_3)\right] \\
& \quad + 2\Re A_{LO}^2 \cos(\omega_8 t - \delta_5 + \delta_2)
\end{aligned}
$$

Since $\omega_4 - \omega_1 = \omega_3 - \omega_6 = \omega_5 - \omega_2 = 2\omega_{LO}$,

$$= 2\Re(A_{LO}^2 + 2A_{IF}^2)\cos\left(\omega_8 t - \frac{2\omega_{LO} L \cdot n(t)}{c}\right)$$

$$= 2\Re(A_{LO}^2 + 2A_{IF}^2)\cos(\omega_8 t - \phi_8) \quad (3\text{-}4)$$

$$I_9^{PD}(t)$$

$$= \Re(E_1 E_5^* + E_1^* E_5) + \Re(E_2 E_6^* + E_2^* E_6)$$

$$= 2\Re A_{LO} A_{IF}[\cos(\omega_9 t - \delta_5 + \delta_1) + \cos(\omega_9 t - \delta_6 + \delta_2)]$$

$$= 2\chi\Re A_{LO} A_{IF}\left[\cos\left(\omega_9 t + \frac{(\omega_1 - \omega_5)L \cdot n(t)}{c}\right) + \cos\left(\omega_9 t + \frac{(\omega_2 - \omega_6)L \cdot n(t)}{c}\right)\right]$$

Since $\omega_1 - \omega_5 = \omega_2 - \omega_6 = -(\omega_{IF} + 2\omega_{LO})$,

$$= 4\Re A_{LO} A_{IF} \cos\left(\omega_9 t - \frac{(\omega_{IF} + 2\omega_{LO})L \cdot n(t)}{c}\right)$$

$$= 4\Re A_{LO} A_{IF} \cos(\omega_9 t - \phi_9) \quad (3\text{-}5)$$

$$\omega_7 = 2\omega_{LO} - \omega_{IF}$$

$$\omega_8 = 2\omega_{LO}$$

$$\omega_9 = 2\omega_{LO} + \omega_{IF} \quad (3\text{-}6)$$

In Eqn. 3-3, 3-4 and 3-5, ϕ_i (i=7, 8, and 9) is the delayed phase of the mm-wave and means the phase drift if the refractive index, n(t), varies randomly with time. It should be underlined that the power of the mm-wave does not fluctuate though n(t)

varies randomly. Only the phase of the mm-wave is changed when n(t) varies with time.

Now, the detected 3 mm-wave components are radiated through wireless channel and received by a mobile station in which these mm-wave components are down-converted by a local oscillator whose frequency is the mm-wave frequency ($2\omega_{LO}$). Then, the obtained IF signal is expressed by

$$\begin{aligned} P_{IF}(t) &= P_0\left[\cos\left(\omega_{IF}t - \frac{(\omega_{IF}+2\omega_{LO})L\cdot n(t)}{c}\right) + \cos\left(\omega_{IF}t - \frac{(\omega_{IF}-2\omega_{LO})L\cdot n(t)}{c}\right)\right] \\ &= 2P_0\cos\left(\frac{2\omega_{LO}L\cdot n(t)}{c}\right)\cdot\cos\left(\omega_{IF}t - \frac{2\omega_{IF}L\cdot n(t)}{c}\right) \\ &= 2P_0\cos\left(\frac{2\omega_{LO}L\cdot n(t)}{c}\right)\cdot\cos\left(\omega_{IF}t - \phi_{IF}\right) \end{aligned} \quad (3\text{-}7)$$

In Eqn. 3-7, ϕ_{IF} is the arbitrary phase noise and does not have to do with the IF signal fading. And $\cos\left(\frac{2\omega_{LO}L\cdot n(t)}{c}\right)$ determines the power of the IF signal and is originated from the phase difference of the local oscillators between the CS and the MS as discussed previously. Evidently, the phase difference results from the fiber-optic transmission. If the refractive index varies with time, the phase difference also varies and the power of the IF signal is to fluctuate with time, i.e. the IF signal fading occurs. However, when the refractive index is constant, $\cos\left(\frac{2\omega_{LO}L\cdot n(t)}{c}\right)$ does not mean the IF signal fading but the only power penalty.

B. Ambient temperature effect

In a laboratory, the circulation of atmosphere and temperature change may have some periods of several minutes according to the environmental conditions such as the time of a day, air pressure, temperature, and so on. In this subsection, the effect of ambient temperature on the IF signal fading is analyzed. Ambient temperature changes may cause the fiber index to slightly vary with time and the phase difference is to have randomness.

Firstly, for the theoretical analysis, two concepts are defined. Thermo-optic coefficient (TOC) is defined to explain the dependence of the temperature change on the refractive index variation. Conveniently, TOC can be expressed by dn/dT which means the change of index when the temperature increases by 1°C. The value of TOC depends on the kind of the optical fiber.

Secondly, it needs to define the IF signal fading factor. That is equivalent with the ratio of the IF signal power when with and without signal fading. This concept is similar to power penalty, but is not the same thing in that the amount of the signal fading is not constant and even varies with time.

Thus, IF signal fading factor induced by ambient temperature can be expressed as follows.

$$\gamma_{IF} = \frac{\cos^2\left(\dfrac{2\omega_{LO} L \cdot (n_0 + \dfrac{dn}{dT} \cdot \Delta T)}{c}\right)}{\cos^2\left(\dfrac{2\omega_{LO} L \cdot n_0}{c}\right)} \tag{3-8}$$

It is known that the refractive index of the practical SMF changes approximately by $10^{-6} \sim 10^{-5}$ if temperature changes by 1°C [15]. For example, Fig. 3-4 shows the simulation result with increasing the temperature when $\frac{dn}{dT} = 10^{-6}$. In Fig 3-4a, when f_{LO} is larger, IF signal fading occurs severely. And Fig. 3-4b shows that the IF fading appears more strongly when the fiber length is longer.

Finally, the simulation results are experimentally examined. The method of the experiment is qualitatively performed because it is hard to measure the temperature of the optical fiber and the entire fiber of 20km can not be heated uniformly, that is to say, only some parts of the fiber can be heated. Thus, the experimental result is compared only qualitatively with simulation results. Experimental setup is similar to one as shown in Fig. 3-1 but at this time, the fiber is heated with common hair dryer. This heating device increases the temperature of the optical fiber by several degrees. The result of the monitoring spectrum analyzer shows that the IF signal power fluctuates with full range from maximum (-30dBm) to minimum value (-60dBm) in a half second. The period of the IF signal fading is considerably shortened to a half second in comparison with several minutes in case of no additional heating process.

To protect the optical fiber from overheating, the fiber is heated for only 10 seconds. Although some parts of the optical fiber is heated, the IF signal fading occurs rapidly in time period. These experimental results show that ambient temperature changes can induce the change of the effective fiber length. And this change of the effective fiber length is the cause of the phase drift which results in the IF signal fading.

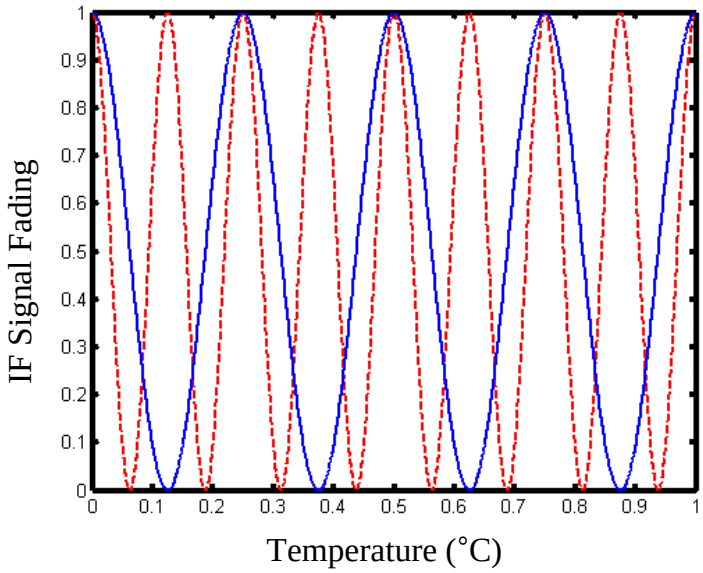

(a) f_{LO} dependence (solid: 15GHz, dash: 30GHz) with fixed L=20km

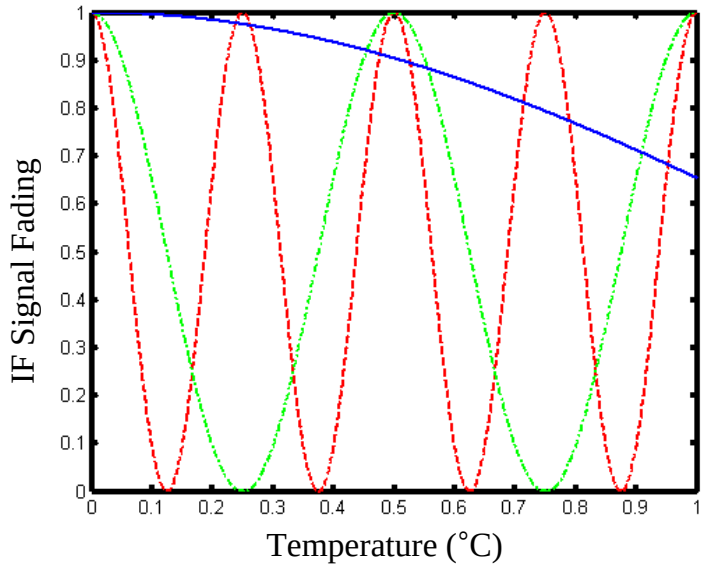

(b) L dependence (solid: 1km, dash&dot: 10km, dash: 20km) (f_{LO} =15GHz)

Figure 3-4 Fiber ambient effects induced fading factor of the IF signal

4. Solution for the IF Signal Fading

The received mm-wave signals are expressed by Eqn. 3-3, 3-4, and 3-5, respectively. If applying the RF bandpass filter (BPF) centered at the frequency of the upper sideband, $\omega_9 = 2\omega_{LO} + \omega_{IF}$, both components of ω_7 and ω_8 are removed and only the ω_9 component is remained. It is the case that the image components are completely removed. In that case, Eqn. 3-7 is rewritten by

$$P_{IF}(t) = P_0 \cos\left(\omega_{IF} t - \frac{(\omega_{IF} + 2\omega_{LO})L \cdot n(t)}{c} \right) \tag{3-9}$$

Although there exists the phase noise, the term of an IF signal fading are removed. The phase drift of the received mm-wave due to the fiber-optic transmission does not affect the amplitude of the IF signal but the phase. Eventually, the RF BPF removes the phenomenon of the IF signal fading by filtering image components of the mm-wave. Even effective length changes of the optical fiber is no problem to the IF signal. The clock recovery circuit after the photodiode, of course, can be the solution for the IF signal fading, but the circuit operating over 60GHz band is practically and economically not the case for the solution. Thus, the RF BPF is the best solution for the IF signal fading problem. The phase noise in the Eqn. 3-9 can be settled down by using a clock recovery circuit operating at the IF band, 1GHz or below, which is manageable band for implementation. In conclusion, the use of the BPF at 60GHz

mm-wave band removes the IF signal fading problem and the use of the clock recovery circuit at IF band settles down the phase noise problem of the IF signal.

To vindicate the effect of the BPF on the IF signal fading, the experiment is the same as Fig. 3-1 except the 60GHz BPF after the photodiode. Since the usable BPF in the laboratory has the center frequency of 60GHz, the frequency of the upper sideband should be 60GHz. Thus, the LO frequency is set to 29.25GHz and the IF frequency to 1.5GHz. In brief, $\omega_7 = 2\omega_{LO} - \omega_{IF} = 57GHz$, $\omega_8 = 2\omega_{LO} = 58.5GHz$, and $\omega_9 = 2\omega_{LO} + \omega_{IF} = 60GHz$. In this frequency band scheme, only the upper sideband is successfully filtered. Fig. 3-5 shows the spectrum of the detected mm-wave signals right after the photodiode and the RF amplifier. Due to the RF amplifier whose gain bandwidth is centered at 60GHz, the amplitude of the upper sideband is larger than any other components. Fig. 3-6 shows the spectrum of the detected mm-wave signals after the 60GHz BPF. Certainly, the upper sideband only remains in the spectrum. With all considerable lapse of time, the IF signal fading phenomenon does not appear to the spectrum analyzer.

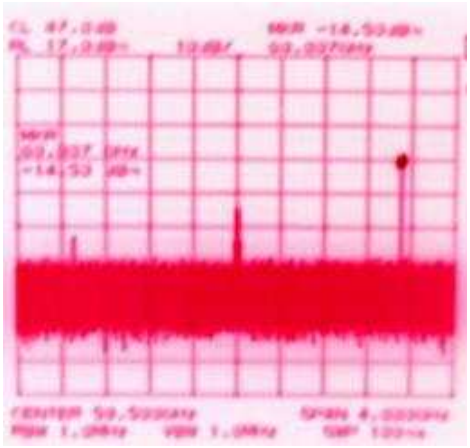

Figure 3-5 Millimeter wave spectrum before the 60GHz BPF

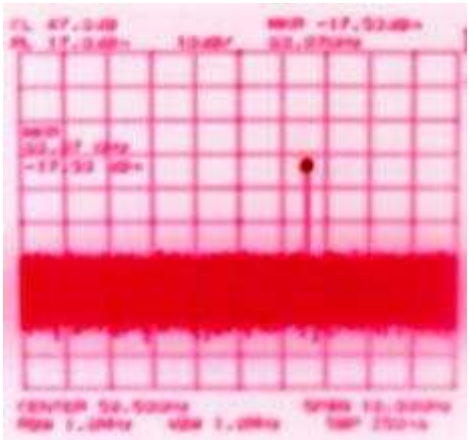

Figure 3-6 Millimeter wave spectrum after the 60GHz BPF

5. System Demonstration

As discussed previously, the simulation of signal fading and the experiment of the system prove that the fiber-optic mm-wave system can operate stably despite the phase drift due to the fiber-optic transmission and ambient conditions. Finally, the system is demonstrated with the IF data using 16QAM (Quadrature Amplitude Modulation) baseband modulation. This IF data is modulated with the IF band carrier of 1GHz. The IF data and carrier are mixed with the 29.5GHz LO carrier. Evidently, the frequency band of the mm-wave is twice the LO carrier, 59GHz. In detail, the experimental setup is shown in Fig. 3-7. To minimize the distortion in the RF mixer, 30GHz BPF is used in the central station. The power of IF source and LO source is -20dBm and -12dBm, respectively. Fig. 3-8 shows the spectrum of the RF carriers which are composed of the LO carrier in 29.5GHz and two IF sideband carrier in 28.5GHz and 30.5GHz. Due to the 30GHz BPF, the lower sideband of IF carrier in 28.5GHz is attenuated as shown in Fig. 3-8a. These RF carriers are modulated in the MZM and transmitted through the SMF of 20km length. In the start point of the fiber-optic transmission, EDFA amplifies the optical carriers. After transmission, the optical carriers are detected by a 60GHz photodiode and amplified and filtered in order to reject the center carrier and lower sideband of the detected mm-wave. Fig. 3-9 shows the spectrum of the 60GHz band which still includes the 16QAM data. After that, the only remained component in 60GHz is down-converted by mixer to the IF band. Fig. 3-10 shows the spectrum of IF band. This IF signal is inserted to the

vector signal analyzer and the result of the transmission of the entire link is demonstrated by error vector magnitude (EVM). The EVM result is shown in Fig. 3-11. And signal constellation and eye pattern are also shown in Fig. 3-11. From the results in Fig. 3-11, the system performance can be assumed to be very stable. EVM is measured to 5.53% and SNR is 23dB. The entire link of the millimeter wave system is successfully demonstrated with the result of 5.53% EVM.

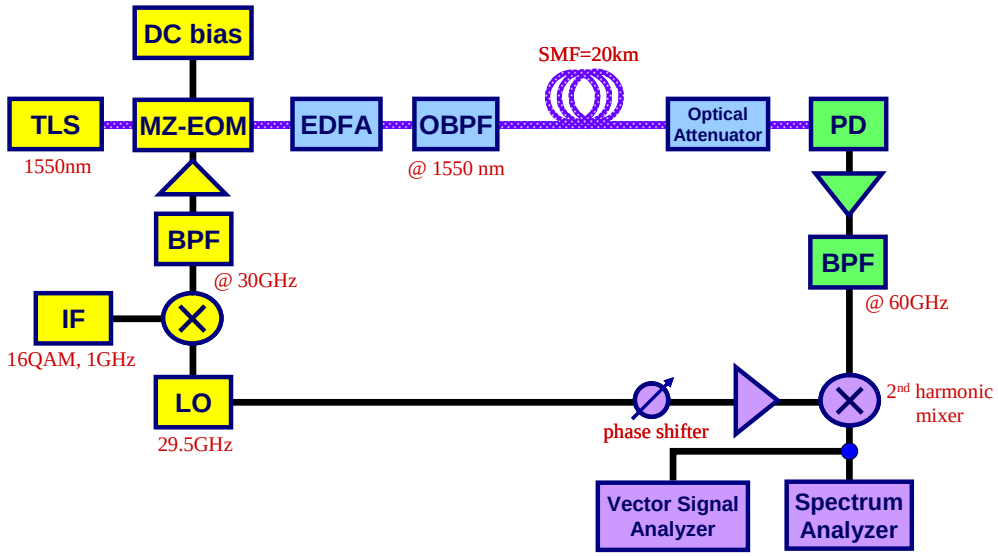

Figure 3-7 Experimental setup with 16QAM data

TLS : Tunable Laser Source

MZ-EOM : Mach-Zehnder electro-optic modulator

EDFA : Erbium-doped fiber amplifier

OBPF : Optical Band Pass Filter

PD : Photodiode

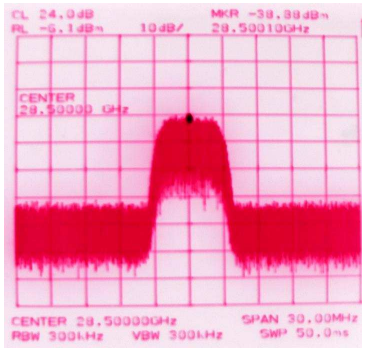

(a) 28.5GHz

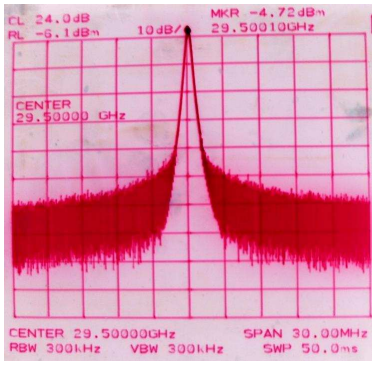

(b) 29.5GHz

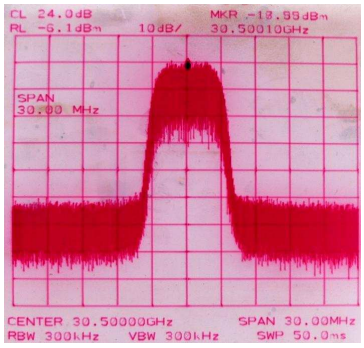

(c) 30.5GHz

Figure 3-8 Spectrum of the RF carriers

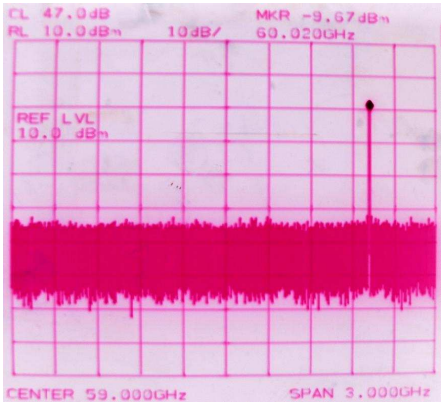

(a) Wide view

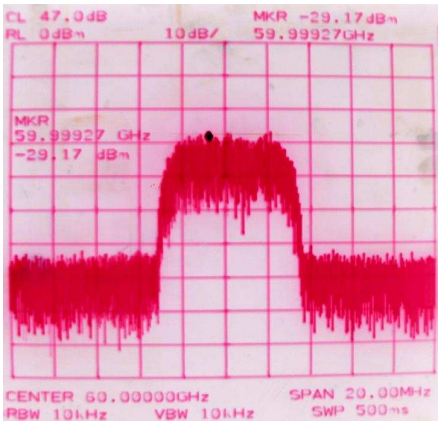

(b) Narrow view

Figure 3-9 Spectrum of the 60GHz mm-wave

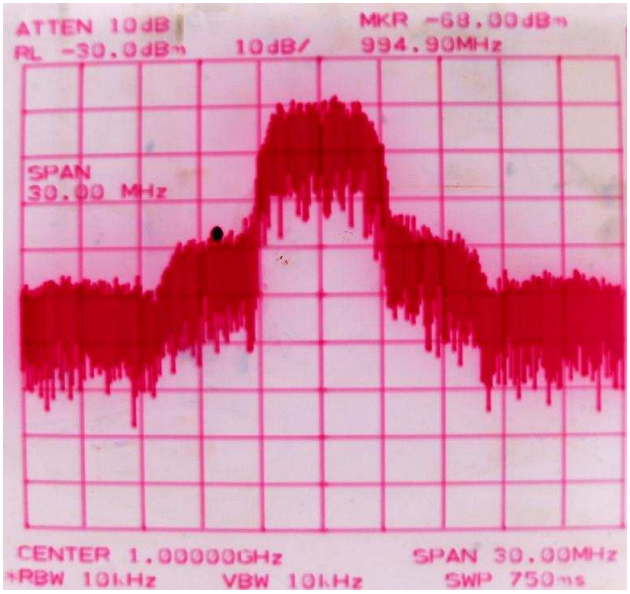

Figure 3-10 Spectrum of the IF band (1GHz)

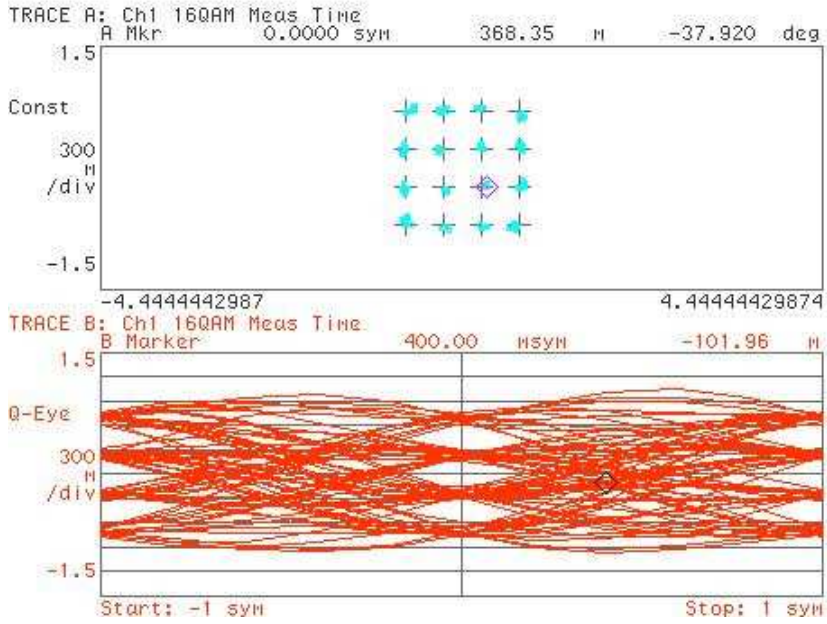

EVM	= 5.5327	%rms	14.670	%	pk at sym	14	
Mag Err	= 3.3275	%rms	-10.682	%	pk at sym	14	
Phase Err	= 4.7678	deg	14.385	deg	pk at sym	58	
Freq Err	= 420.28	Hz					
IQ Offset	= -46.243	dB	SNR (MER)	= 22.965		dB	
Quad Skew	= -509.47	mdeg	Gain Imb	= -0.103		dB	

Figure 3-11 Error vector magnitude (EVM) result

IV. Conclusion

In this thesis, the fiber-optic millimeter wave system using self-heterodyne method is demonstrated by theory and experiment. The entire link of the system includes central station, fiber-optic channel, base station, and mobile station. In the central station, the dual optical carriers whose frequencies are separated by the desired mm-wave frequency are generated. The fiber-optic channel is composed of the 20km SMF, EDFA, optical bandpass filter, and optical attenuator. In the base station, the dual optical carriers are detected by a photodiode and mm-wave is generated by the optical self heterodyne detection method. This optically generated mm-wave is down-converted to the IF band by a local oscillator in the mobile station.

In the system described above, this thesis highlights the phenomenon of signal fading in IF band which is theoretically analyzed in III.3. If considering the practical length of the fiber-optic channel is less than 20km, it is assumed that the chromatic dispersion and the PMD do not have great influence on the signal quality. Thus, the environmental conditions can cause the effective length of the optical fiber to vary with time. Because of the effective fiber-length changes, the phase difference between the central station and the mobile station becomes not fixed but arbitrary, and the phase drift which is the direct origin of the IF signal fading occurs. To reduce the IF signal fading, it is necessary to reject the image components by using 60GHz BPF or adopt the additional clock recovery circuit after the photodiode in the base station. In

the chapter III.4, the 60GHz BPF is selected for the solution of the IF signal fading because the clock recovery circuit operating at 60GHz band is not practical.

In the chapter III.5, the fiber-optic millimeter wave system is demonstrated with the 60GHz BPF after the photodiode and 16QAM baseband modulation. To evaluate the performance of the system, the EVM factor is introduced and has the value of 5.53%.

In conclusion, the fiber-optic 60GHz millimeter wave system using optical self heterodyne detection method is successfully demonstrated with adoption of the 60GHz BPF. The origin and the solution of the IF signal fading problem is theoretically and experimentally analyzed. The performance of the system shows the 5.53% EVM result and the signal constellation and eye pattern of 16QAM data also show the error-free transmission results.

References

[1] T. Kuri, and K. Kitayama, “Optical heterodyne detection technique for densely multiplexed millimeter-wave-band radio-over-fiber systems,” J. of Lightwave Technology, vol. 21, pp. 3167-3179, Dec. 2003.

[2] H. Schmuck, and R. Heidemann, “Hybrid fiber-radio field experiment at 60GHz,”in Proc. ECOC’96, Oslo, Norway, nol. ThC1.2, pp. 4.59-4.66, 1996.

[3] K. Kitayama, “Architectural considerations on fiber radio millimeter-wave wireless access systems,”J. Fiber Interat. Opt., vol. 19, pp. 167-186, 2000.

[4] H. Ogawa, D. Polifko, and S. Banda, “Novel techniques for high-capacity 60GHz fiber-radio transmission systems,” IEEE Tans. Microwave Theory Tech., vol. 40, pp. 2285-2293, Dec. 1992.

[5] D. Novak, Z. Ahmed, R. B. Waterhouse, and R. S. Tucker, “Signal generation using pulsed semiconductor lasers for application in millimeter-wave wireless links,” IEEE Trans. Microwave Theory Tech., vol. 43, pp. 2270-2276, Sept. 1995.

[6] Y. Doi, S. Fukushima, T. Ohno, Y. Matsuoka, and H. Takeuchi, “Phase shift keying using optical delay modulation for millimeter-wave fiber-optic radio links,” J. Lightwave Technol., vol. 18, pp. 301-307, Mar. 2000.

[7] H. Harada, K. Sato, and M. Fujise, “A radio-on-fiber based millimeter-wave road-vehicle communication system by a code division multiplexing radio transmission scheme,” IEEE Trans. Intell. Trans. Syst., vol. 2, pp. 165-179, Dec. 2001.

[8] G. Grosskopf, D. Rohde, R. Eggermann, S. Bauer, C. Bornholdt, M. Mohrle, and B. Sartorius, “Optical millimeter-wave generation and wireless data transmission using a dual-mode laser,” IEEE Photon. Technol. Lett., vol. 12, pp. 1692-1694, Dec. 2000.

[9] Y. Shoji and H. Ogawa, “Experimental demonstration of 622 Mbps millimeter-wave over fiber link for broadband fixed wireless access system,” in 2002 Int. Topical Meeting Microwave Photonics(MWP2002) Tech. Dig., vol. F3-2, Awaji, Huogo, Japan, Nov. 2002, pp. 367-370.

[10] S. C. Rashleigh, “Origins and control of polarization effects in single-mode fibers,” J. Lightwave Technol., vol. LT-1, pp. 312-331, Jun. 1983.

[11] K. Kitayama, “Ultimate performance of optical DSB signal-based millimeter-wave fiber-radio system: effect of laser phase noise,” J. Lightwave Technol., vol. 17, pp. 1774-1781, Oct. 1999

[12] J. M. Fuster, J. Marti, J. L. Corral, V. Polo, and F. Ramos, “Generalized study of dispersion-induced power penalty mitigation techniques in millimeter-wave fiber-optic links,” J. Lightwave Technol., vol. 18, pp. 933-940, Jul. 2000.

[13] R. Hofstetter, H. Schmuck, and R. Heidemann, “Despersion effects in optical millimeter-wave systems using self-heterodyne method for transport and generation,” IEEE Trans. Microwave Theory and Techniques, nol. 43, pp. 2263-2269, Sep. 1995.

[14] U. Gliese, S. Norskov, and T. N. Nielsen, “Chromatic dispersion in fiber-optic microwave and millimeter-wave links,” IEEE Trans. Microwave Theory and

Techniques, vol. 44, pp. 1716-1724, Oct. 1996.

[15] P. S. Andre, A. N. Pinto, J. L. Pinto, “Effect of temperature on the single mode fibers chromatic dispersion,” Microwave and Optoelectronics Conference, 2003. IMOC 2003. Proceedings of the 2003 SBMO/IEEE MTT-S International, vol. 1, pp. 231-234, 2003.

국 문 요 약

자기-헤테로다인 방식을 이용한 밀리미터파 광전송 시스템에서 IF 신호 페이딩에 관한 연구

사용자에게 초고속 데이터의 무선 서비스를 제공하기 위해서 밀리미터파 대역에 대한 관심이 높아지고 있다. 특히, 60GHz 대역의 밀리미터파는 가까운 미래에 다양한 서비스에 이용될 것으로 예상되며, 중앙 네트워크에서 기지국까지의 밀리미터파 전송은 기존의 광전송 시스템을 이용하는 것이 기술적, 경제적으로 매력을 갖는다고 할 수 있다. 본 논문에서는 60GHz의 밀리미터파를 광학적 자기-헤테로다인 방식을 이용하여 생성하고 이를 광전송하는 과정에서 생기는 문제로 인한 IF 신호의 페이딩에 대한 연구를 수행하였다.

주변 환경적 요인으로 인한 광섬유의 굴절률의 랜덤한 변화는 이동국에서 밀리미터파의 주파수 하향변환시 IF 대역의 신호 페이딩으로 나타날 수 있으며, 이에 대한 실험적 관찰 결과, IF 신호의 페이딩은 주기적으로 일어났으며, 시간 주기는 환경적 요인에 따라 다양하게 나타났다. 또한, 신호의 위상성분에 대한 이론적 분석을 통해, 기지국의 광 검출기 뒤에 60GHz 대역통과필터를 접속하여 영상 신호를 제거하면, IF 대역 신호의 페이딩 문제를 해결할 수 있음을 알 수 있었다.

또한, 광학적 자기-헤테로다인 방식을 이용한 밀리미터파 광전송 시스템의 전

송 결과를 시현하기 위해, 16QAM의 데이터를 IF 대역에 변조하였으며, 결과적으로 IF 신호의 페이딩 없이 성공적으로 전송됨을 실험을 통해 검증하였다.